Available online at www.sciencedirect.com
ScienceDirect
Food Chemistry 106 (2008) 56–64
Food Chemistry
www.elsevier.com/locate/foodchem

Protein and water structural changes in fish surimi during gelation as revealed by isotopic H/D exchange and Raman spectroscopy

Ignacio Sánchez-González [a], Pedro Carmona [b], Pilar Moreno [a], Javier Borderías [a], Isabel Sánchez-Alonso [a], Arantxa Rodríguez-Casado [b], Mercedes Careche [a,*]

[a] *Instituto del Frío-CSIC, c/José Antonio Novais 10, 28040 Madrid, Spain*
[b] *Instituto de Estructura de la Materia-CSIC, c/Serrano 121, 28006 Madrid, Spain*

Received 30 October 2006; received in revised form 6 March 2007; accepted 17 May 2007

Abstract

Structural changes of proteins and water during gelation of fish surimi, have been studied by isotopic H/D exchange of water and Raman spectroscopy assisted by monitoring of rheological characteristics, in order to get insights into the structural and functional properties of surimi gels. The results indicate the following: (i) Protein hydrogen bond rearrangements occur involving mainly α-helix to β-sheet transition, (ii) the relative intensity of the symmetric H_2O stretching band near 3220 cm^{-1} tends to decrease upon gelation, (iii) H/D exchange reveal a slower deuteration kinetics in the gels as compared to the surimi, (iv) the low temperature scanning electron microscopy shows a smaller pore size of the gel network as compared to the surimi, and suggests that water domains in gel are more inaccessible to D_2O, which is consistent with higher water holding capacity in the gel.

Keywords: Fish surimi; Gel; Water structure; Protein structure; H/D exchange; Raman spectroscopy; Alaska pollock; Southern blue whiting

1. Introduction

Surimi, the stabilized myofibrillar protein that is obtained from mechanically deboned fish flesh, is washed, mixed with cryoprotectans, and stored frozen, is used as a raw material in order to obtain a great variety of products. This is due to the unique gelling properties of the myofibrillar proteins. The gelling process entails the association of long myofibrillar protein chains which produce a continuous three-dimensional network in which water and other components are trapped. As a result, a viscoelastic gel is obtained.

A general description of the protein–protein and water–protein interactions involved during the gelling process has been established, and to some extent, the order of interaction of the (acto)myosin molecule has been outlined. This interaction mostly uses isolated protein or protein fragment preparations, sol suspensions at relatively low protein concentration or, by dissolving the gels and analysing their structure (For reviews see e.g. An, Peters, & Seymour, 1996; Lanier, Carvajal, & Yongsawatdigul, 2005; Niwa, 1992; Stone & Stanley, 1992). In general terms, salt addition to surimi, with sufficient degree of grinding, breaks ionic bridges within the proteins, dissolves them and destabilizes their molecular structure toward subsequent thermal denaturation and promotes hydrophobic interaction. These hydrophobic interactions, rearrangement of hydrogen bonds as well as covalent bonds of proteins, play important roles in the formation of the protein network when the sol is heated. However, there is still some uncertainty about the precise mechanism responsible for gel formation. This is in part due to less work dealing with the analysis *in situ* of the structural changes occurring on the surimi proteins (Bouraoui, Nakai, & Li-Chan, 1997; Thawornchinsombut, Park, Meng, & Li-Chan, 2006), and on the structure and mobility of water during the gelation process.

* Corresponding author. Tel.: +34 91 5445607; fax: +34 91 5493627.
E-mail address: mcareche@if.csic.es (M. Careche).

0308-8146/$ - see front matter © 2007 Published by Elsevier Ltd.
doi:10.1016/j.foodchem.2007.05.067

One way to study the molecular changes in proteins and water in food systems, is by using vibrational spectroscopy. In particular, Raman spectroscopy gives information based on both the relative intensity and frequencies of vibrational motions on the aminoacid side chains, polypeptide backbone, and the structure and mobility of water. Raman spectroscopy has been considered as a useful tool to investigate molecular interactions and changes in proteins (Careche, Herrero, Rodriguez-Casado, Del Mazo, & Carmona, 1999; Herrero, Carmona, & Careche, 2004) and water (Herrero, Carmona, Garcia, Solas, & Careche, 2005) of fish muscle during frozen storage, as well as in the study of the changes in the side chains of polypeptide skeleton and secondary structure during gelation of surimi *in situ* (Bouraoui et al., 1997) or isolated actomyosin (Ogawa et al., 1999).

Based on Raman studies of *in situ* structural changes of proteins in Pacific whiting surimi, and during different gelling conditions, Bouraoui et al. (Bouraoui et al., 1997) proposed that protein changes observed in the Raman spectra may be related to the gel strength and fold score. In particular, the changes in intensity of Raman band near 530 cm^{-1} were attributed to either involvement of disulfide bonds and/or hydrophobic interactions in gel formation. Changes in secondary structure were more pronounced after the cooking treatments and differed for gels prepared with or without setting. Other features, included changes in the tyrosine doublet ratio, frequency downshifting as well as intensity decrease of the Raman band assigned to C–H stretching vibration of aliphatic residues.

The spectral features of the Raman spectrum of water, based on studies in solutions of biological macromolecules and biological systems (Lafleur, Pigeon, Pézolet, & Caillé, 1989; Maeda & Kitano, 1995; Walrafen & Fisher, 1986) can be summarized as follows: (a) the band between 3100 and 3500 cm^{-1} attributable to O–H stretching motions and (b) the low frequency range (below 600 cm^{-1}), related to intermolecular water and protein librations and restricted translational motions involving the bending and stretching vibrations of the O(N)–H···O(N) units.

The objective of this work was the study of the structural changes of proteins and water during surimi gelation by Raman spectroscopy. This was performed along with the monitoring of the rheological and other physical chemical characteristics of resulting gel products, as well as the microstructure of the surimi and gels, in order to obtain more insights into the surimi gelation process.

2. Materials and methods

2.1. Species

Alaska pollock (*Theragra chalcogramma*) surimi (grade FA) from the North Pacific, was purchased from a local supplier (Angulas Aguinaga S.A, Spain) and stored at −20 °C prior to use (6–9 months after capture date). Southern blue whiting (*Micromesistius australis*) surimi (grade FA) from the South-West Atlantic was purchased (Patagonia y Antártida S.A, Argentina), stored at −20 °C and used within 9–11 months after capture. The shelf life of these lots was 18–20 months at a maximum temperature of −18 °C.

2.2. Surimi gel preparation

Surimi stored at −20 °C was partially thawed at room temperature for 1 h. It was cut in to small pieces where approximately 800 g was chopped in a vacuum cutter for 2.5 min (Stephan Universal Machine UM5, Stephan u. Söhne GmbH & Co., Germany), and mixed for 2.5 min with enough NaCl and water for a final formulation with 74.5% moisture, 2.5% NaCl and 17% protein. This was defined as sol. The temperature was kept below 10 °C. A portion of the sol was stored at 2 °C for subsequent analyses, and the rest was placed into polyvinilidine casings (Amcor flexible Hispania, Spain) and subjected to heating at 90 °C for 50 min in a water bath, to obtain the cooked gels. These gels were cooled in iced water and stored at 2 °C before analysis. Four gels of about 190 g (35 mm diameter $x \sim 15$ cm length) were obtained, and used for subsequent analyses.

2.3. Isotopic H/D exchange

Portions of surimi and gels of 2.0 cm length and ~5.0 mm diameter were transferred to glass tubes (2.0 cm length) open on both ends. Samples were closed with a dialysis membrane (SnakeSkin PLEATED dialysis tubing 3500 mwco. Pierce, Perbio USA). Tubes were covered with an excess of deuterium oxide (99.9 at.% D, Aldrich) and maintained at 15 °C for 7 h in a water bath. Each hour one tube was taken for FT-Raman analyses, performed as described in the corresponding section.

2.4. Proximate analyses

For analysis of the moisture content, 5.0 g of sample were introduced in an aluminium sample holder and kept in a forced air draft oven at 105 °C over 24 h until a constant weight was achieved. Results were expressed in grams of water per 100 g of sample. Assays were made in triplicate for each sample (Surimi, sol or gel). Protein determination was carried out in triplicate by the Dumas combustion method in a Leco CNS 2000 instrument (St. Joseph, MI, USA). This method converts covalently bound nitrogen into nitrogen gas which is quantified by passing the gas through a conductivity cell. Samples were measured in triplicate and expressed in % protein using 6.25 as protein nitrogen conversion factor (AOAC, 1995).

2.5. Water holding capacity (WHC)

The water holding capacity was measured by a modification of Roussel and Cheftel's (Roussel & Cheftel, 1990)

method. A 3.0 g of surimi, sol or cooked gel was introduced into centrifuge tubes with two micropipette filters (Gilson Pipetman) and was centrifuged at 1830*g* (Heraeus L-R, Kendro Loratory Products, Germany) for 15 min at room temperature. Results were expressed as grams of water retained in the sample per 100 g of water present in the sample before centrifugation (%). Measurements were made in triplicate.

2.6. Folding test

This was carried out according to the National Fisheries Institute procedure (Lanier et al., 1991). Gels were assigned to five classes: AA, A, B, C or D, ranging from AA (good quality, score 5) to D (poor quality, score 1). At least 3 determinations were performed per gel.

2.7. Textural profile analysis (TPA)

The assays were performed using a TA.XT2i SMS Stable Micro Systems Texture Analyzer (Stable Microsystems Ltd. Surrey, England) on cylindrical cores of 35 ± 1 mm diameter and 30 ± 1 mm length. TPA assay was achieved in gels by compressing 50% using a load cell of 25.0 kg at a compression speed of 60 mm min^{-1} and a 75 mm diameter cylindrical probe. Hardness, springiness, cohesiveness and chewiness were measured and defined as reported by Uresti and others (Uresti, López-Arias, González-Cabriales, Ramirez, & Vázquez, 2003).

2.8. Stress-relaxation test

This was performed in surimi and gels using the same texturometer as above. The samples were compressed by 10% with a 75 mm diameter cylindrical probe and a load cell of 5.0 Kg at a crosshead speed of 0.8 mm s^{-1}, the deformation being kept constant for 600 s. Initial stress (σ_0) was obtained; relaxation of stress was monitored as a function of time and the curves were fitted to the Maxwell model (Mohsenin, 1970):

$$\sigma(t) = \sigma_e + \sigma_1 e^{-t/T_1} + \sigma_2 e^{-t/T_2} + \sigma_3 e^{-t/T_3}$$

where $\sigma(t)$ is the decaying stress, σ_e is stress at equilibrium ($t = \infty$), σ_1, σ_2, and σ_3 are the decay stress of each exponential, and T_1, T_2, and T_3 the relaxation times. For each fitting, starting T_i and σ_i values included into the nonlinear regression equation were: $T_1 = 200$, $T_2 = 20$, $T_3 = 2$, and σ_e, σ_1, σ_2, $\sigma_3 = 0.3$ times σ_0. The viscous and elastic moduli (η_i and E_i respectively) were calculated taking into account that $T_i = \eta_i/E_i$, and $\sigma_i = E_i *$Deformation.

2.9. FT-Raman spectroscopy

Surimi, sol and gels were transferred to glass tubes (5.0 cm height and 5.0 mm i,d; Wilmad Glass co., Inc., Buena, NJ). Spectra were excited with a 1064 nm Nd:Yag laser line and recorded on a Bruker RFS 100/S FT spectrometer. The scattered radiation was collected at 180° to the source, and the frequency-dependent scattering of the Raman spectra that occurs with this spectrometer was corrected by multiplying point by point $(\nu_{laser}/\nu)^4$. Raman spectra were resolved at 4.0 cm^{-1} resolution with a liquid nitrogen-cooled Ge detector. The samples thermostated at 15–20 °C were illuminated with 290 mW laser power.

Amide I band (around 1650 cm^{-1}) was used to estimate the secondary structure composition (Alix, Pedanou, & Berjot, 1988) and was measured as reported previously (Herrero et al., 2004). Normalization against the Raman band of phenylalanine near 1003 cm^{-1}, considered to be invariable during conformational changes of proteins, was used as an internal standard of the spectra. The intensity ratio of I_{850}/I_{830} doublet bands was used to monitor the microenvironment around tyrosine residues (Li-Chan, Nakai, & Hirotsuka, 1994; Siamwiza et al., 1975). The C–H stretching mode of aliphatic amino acid residues (2935 cm^{-1}) was also studied according to Bouraoui et al. (1997) with Phe as internal standard. A total of six thousand scans per replicate, consisting of three separate samples of two thousand scans, were recorded. This prevents ageing of the sample due to prolonged exposure to the laser beam and averages any acquisition variability due to instrument conditions.

The O–H stretching region (3100–3500 cm^{-1}) was analyzed in order to report the structural changes in water. In order to obtain information on the sizes of interstitial water domains, of sizes below 15 nm, the intensity near 3220 cm^{-1}, normalized in relation to the 3400 cm^{-1} intensity, was measured according to Lafleur et al. (1989) These authors stated that the smaller the 3220/3400 intensity ratio of the symmetric and asymmetric νOH bands, the smaller the water domain sizes. On the other hand, the intensities at 3185, 3160, and 3140 cm^{-1} relative to that of the maximum near 3220 cm^{-1} were also measured as an indication of the hydrogen bonding strength in water (Scherer, 1980; Sammon, Bajwa, Timmins, & Melia, 2006).

In the H/D exchange experiments, the O–H stretching region was used. The maxima of the C–H and O–H stretching bands in the 2800–3500 cm^{-1} region were obtained by curve fitting, which was achieved for each 2000 scans, starting with maxima near 2935 cm^{-1} and 3220 cm^{-1}, and considering 150 cm^{-1} bandwidth. Maximum frequency of the O–H stretching band and the relative O–H/C–H area in the course of deuteration were recorded. Deuteration kinetics in each case, was plotted as water fraction unexchanged as a function of H/D exchange time, this fraction being defined as the O–H/C–H area ratio divided by the value of this ratio at time 0. For deuteration measurements as a function of time, every graphics point results from the average of three replicates, each of them being recorded with 2000 scans.

Spectra were processed and evaluated using Grams/AI (Thermo Electron Corporation, USA) and Opus 2.2. (Bruker, Karlsruhe, Germany) software.

2.10. Low-temperature scanning electron microscopy (LT-SEM) analysis

The surimi and gel samples were kept in the fully hydrated state and then fixed mechanically onto the specimen holder of an Oxford CT1500 cryotransfer system. This instrument plunge-freezes the samples in subcooled liquid nitrogen and then transfers them to the preparation unit, where they are fractured. The samples were coated by gold sputtering and examined on the cold stage of a DSM 960 Zeiss SEM microscope.

2.11. Experimental design

The first series of experiments were conducted with Alaska pollock surimi. FT Raman analyses of surimi, sol and gel were performed, along with parameters such as proximate composition, water holding capacity, folding test, TPA and compression relaxation tests. Each experiment consisted in the preparation of gels and measurements of all the parameters listed above (first day) as well as the FT Raman analysis (second day). Three experiments were carried out in three separate days and results from each day were considered as a replicate.

In order to obtain better insight into the structure and properties of water, a H/D exchange experiment was carried out as well as microstructure analysis. For this second series of experiments, Southern blue whiting was used as a surimi source, using the same experimental set up as before. Three replicated experiments were conducted for each sample (surimi or gel).

2.12. Statistical analysis

One way analysis of variance was performed as a function of type of sample (surimi, sol and gel). The Levene test was used to check the equality of variances. Where variances were equal, the difference between means was analyzed by the Bonferroni test. Where equality of variances could not be assumed a Tamhane T2 test was used. For analysing the differences between two samples, a *t*-student test for independent groups was carried out. For the H/D exchange experiments, linear regression analysis was performed as a function of deuteration time. The statistical package used was SPSS 13 (SPSS Inc, Chicago IL) and significance was established at 0.05 levels. Results were expressed average ± standard error of the mean (SEM).

3. Results

3.1. Experiment 1: Physical-chemical properties of surimi, sol and gels and structural features of protein and water during gelation

3.1.1. Moisture, protein content and WHC

The moisture and protein contents of the sol and gels were in agreement with the designed formulation, with ~74.5 and 17% moisture and protein, respectively (Table 1). There was a significant increase of the WHC in the gels as compared to surimi or sol. The WHC in the gels was higher than that of Sánchez-Alonso and others (Sánchez-Alonso, Haji-Maleki, & Borderías, 2006). This may be due to the differences in the methodology of measuring WHC, since in our work, micropipettes filters have been used during the centrifugation process, as opposed to filter paper, used by the cited authors.

3.1.2. Folding test, texture profile analysis (TPA), and stress-relaxation test

The fold score was five, and therefore the gels were of good quality. Hardness, springiness, cohesiveness, and chewiness as measured by the TPA assay were respectively: 113.5 ± 1.1 N; 7.30 ± 0.32 mm; 0.44 ± 0.02; 363 ± 5.3 Nmm. These values were in agreement with other authors (Munizaga & Barbosa-Cánovas, 2004; Sánchez-Alonso et al., 2006). Table 2 shows the results of stress-relaxation test in surimi and gels. Initial and equilibrium stress, σ_0 and σ_e, were respectively four and ten times higher in the gels as compared to the surimi. These parameters have been related to cross-links density between protein chains (σ_0) and to residual solidity of the system derived from permanent cross-links (σ_e) (Hamann & MacDonald, 1992). The viscous to elastic constant ratios for each exponential term are reflected in the values for the relaxation times. T_1 and T_2 were significantly higher for the gels, whereas no differences

Table 1
Moisture (%), protein (%), water holding capacity (WHC, %) in Alaska pollock (*Theragra chalcogramma*) surimi, sol and gel (mean ± SEM)

Samples	Moisture	Protein	WHC
Surimi	74.8 ± 0.1^a	17.3 ± 0.3^a	91.9 ± 0.1^a
Sol	74.5 ± 0.4^a	16.3 ± 0.8^a	91.7 ± 0.1^a
Gel	74.1 ± 0.1^a	16.3 ± 0.3^a	96.3 ± 0.1^b

Different letters for each parameter indicate significant differences ($P < 0.05$).

Table 2
Stress-relaxation test in Alaska pollock (*Theragra chalcogramma*) surimi and gels

Parameter	Surimi	Gel
σ_0	2.35 ± 0.10^a	9.77 ± 0.41^b
σ_e	0.28 ± 0.02^a	2.84 ± 0.12^b
E_1	5.8 ± 0.2^a	21.8 ± 1.3^b
E_2	5.7 ± 0.4^a	16.0 ± 0.7^b
E_3	8.1 ± 0.4^a	24.7 ± 1.0^b
η_1	1160 ± 32^a	4747 ± 218^b
η_2	112 ± 7^a	347 ± 16^b
η_3	11.5 ± 0.6^a	37.8 ± 1.8^b
T_1	200 ± 6^a	223 ± 5^b
T_2	19.8 ± 0.2^a	21.8 ± 0.3^b
T_3	1.43 ± 0.04^a	1.53 ± 0.03^a

The parameters are: initial and equilibrium stress (σ_0, σ_e, kPa), elastic moduli (E_1, E_2, E_3, kPa), viscous moduli (η_1, η_2, η_3, kPa s), and relaxation times (T_1, T_2, T_3, s). Results are expressed as mean ± SEM. Different letters for the same parameter indicate significant differences ($P < 0.05$).

were found for T_3. When the values for the gels were fitted to a mono-exponential equation with the residual term, the corresponding parameters extracted were in the same range of those of other authors (Hamann & MacDonald, 1992). The gels had higher viscous elements for η_1 and η_2 and η_3 was higher in the surimi, and the same trend was found for the elastic moduli, E_i.

3.1.3. Protein secondary structure

Fig. 1 shows the amide I band spectra in surimi, sol and gel samples. This band (centred near 1655 cm^{-1}) is correlated with the amount of the types of protein backbone conformation (Alix et al., 1988; Tu, 1982) and consists of overlapped band components falling in the 1658–1650, 1680–1665, and 1665–1660 cm^{-1} ranges which are attributable to α-helices, β-sheets, and random coil respectively (Frushour & Koening, 1975). Comparison of the amide I band of surimi samples reveals a shifting of the band maximum toward higher frequencies in going from surimi to the gels, with more marked changes (around 15.0 cm^{-1}) between the sol and the gel. The estimates of protein secondary structures (Fig. 2) showed that surimi posses a predominant α-helical structure and lesser contribution of β-sheets. The helical structure decrease with concomitant increase in β-sheets that was observed after heating was close to 40%. Significant increases in turns and unordered structures in the gels were also observed. The percentage of α-helix in surimi was higher than that found from other works which report a range between 35% and 53% in these samples (Bouraoui et al., 1997; Moosavi-Nasab, All, Ismail, & Ngadi, 2005; Thawornchinsombut et al., 2006). The differences may be due to different methodologies of calculation of the secondary structure percentages or species differences. The general trend as regards to secondary structure changes upon gelation was similar to that of Bouraoui et al. (1997), although the absolute percentage changes were higher in Pacific whiting surimi gels.

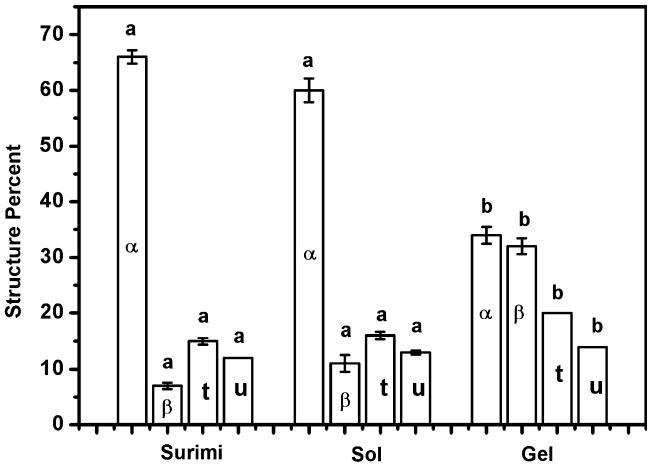

Fig. 2. Protein secondary structure of surimi, sol and gel of Alaska pollock (*Theragra chalcogramma*) (mean ±SEM). The letters inside the bars indicate: α, α-helices; β, β-sheets; t, turns; and u, unordered. Different letters on the bar tops for the same protein structure indicate significant differences ($P < 0.05$).

Fig. 3 shows the amide III band spectra in surimi and gels. This band, which provides additional information of polypeptide backbone (Lippert, Tyminski, & Desmules, 1976; Yu, Lippert, & Peticolas, 1973), is complementary of the amide I. The amide III mode involves N–H in plane bending and C–N stretching as well as contributions from C_α–C stretching and C=O in plane bending, which has been assigned to the 1309 and 1273 cm^{-1} bands which fall in the well established range attributable to α-helices. In surimi, a band at 1306 cm^{-1} is present as a shoulder, which disappeared in the gels. The change in the 1273 cm^{-1} band is indicative of α-helix loss and consistent with the results shown in the amide I region.

3.1.4. C–H stretching region

The band centred around 2938 cm^{-1} is assigned to CH_2 asymmetric and CH_3 symmetric stretching vibrations of

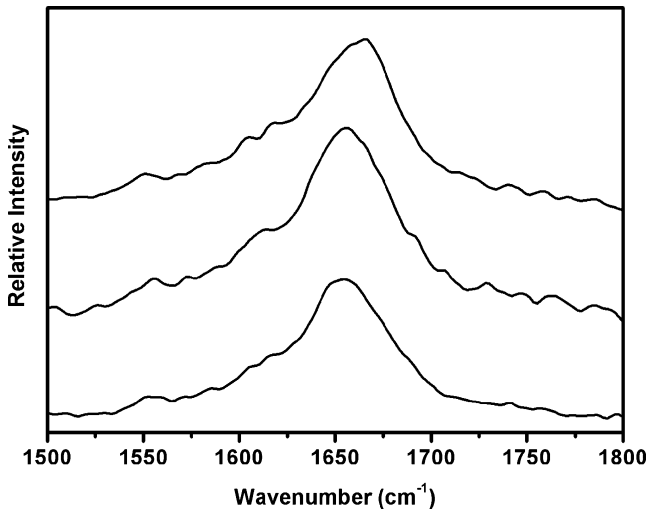

Fig. 1. Amide I Raman spectra of surimi (bottom), sol (middle), and gel (top) of Alaska pollock (*Theragra chalcogramma*).

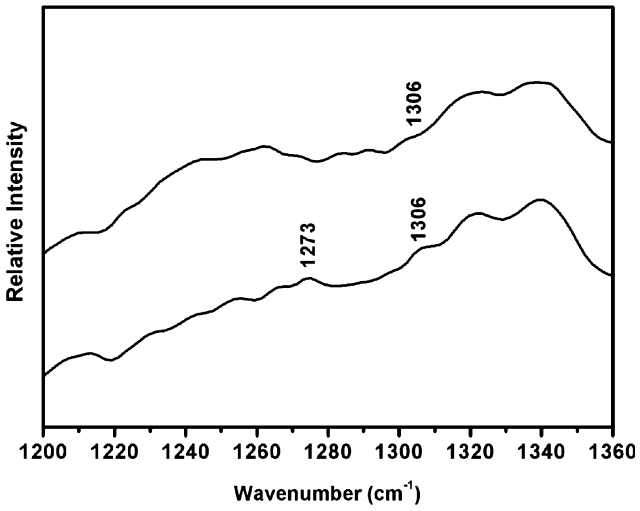

Fig. 3. Amide III Raman spectra of surimi (bottom), and gel (top) of Alaska pollock (*Theragra chalcogramma*).

aliphatic residues. The intensity of this band decreased in the sol and gel compared to the surimi (Table 3), but the high standard errors do not allow to observe significant differences among the samples. This trend was also observed by Bouraoui et al. (1997) who interpreted that this could be due to the environment of aliphatic C–H groups which may be related to hydrophobic interactions during processing of surimi.

3.1.5. Tyrosine doublet (850 and 830 cm^{-1})

The doublet band of tyrosine is assigned to vibrations of the para-substituted benzene ring of tyrosine residues. These are affected by the environment and the involvement of the phenolic hydroxyl group in hydrogen bonding (Li-Chan et al., 1994; Siamwiza et al., 1975). Tyrosine doublet ratio I_{850}/I_{830} cm^{-1} has been reported to decrease upon gelation (Bouraoui et al., 1997) and interpreted as tyrosine becoming buried in a more hydrophobic environment and involved as strong hydrogen bond donors (Li-Chan et al., 1994; Siamwiza et al., 1975). The tyrosine doublet was observed as two faint bands in the FT Raman spectra. A slight, although non significant ($P = 0.07$) decrease in the I_{850}/I_{830} ratio, was observed in going from surimi to sol (Table 3). Nevertheless this result has to be taken with caution, due to the difficulty of the calculation of these band intensities in the present spectra.

3.1.6. O–H stretching region

The vibrations of water molecules include two O–H stretching bands, namely, a symmetric one whose maximum appears around 3220 cm^{-1} and an asymmetric band which appears around 3400 cm^{-1} (Maeda & Kitano, 1995). Table 3 shows a decreasing trend of this intensity from the surimi to the gel, although no significant differences could be found among the samples. Some authors have demonstrated that an increase of the I_{3220}/I_{3440} ratio occurs in going from small water interstices to greater domains of water (Lafleur et al., 1989) when considering domain sizes below 15 nm. The relative intensities at 3185, 3160 and 3140 cm^{-1} also showed a trend to decrease, but with no significant differences among the samples (Table 3). These trends could be interpreted in terms of weaker hydrogen-bonded molecular species of water (Sammon et al., 2006; Scherer, 1980).

3.2. Experiment 2: H/D exchange and LT-SEM microstructure analysis

In order to check the consistency between the previous and the present experiment, a characterization of the techno functional properties of the batch used for the H/D exchange was performed. Moisture (74.5 ± 0.05%), protein (18.6 ± 0.4%), and WHC (97.00 ± 0.4 g/100 g) fell well within the range of the gels used in the former experiment (Table 1). The TPA analysis gave the following values for the hardness (138.9 ± 8.5 N), springiness (7.30 ± 0.04 mm), cohesiveness (0.47 ± 0.01), and chewiness (477 ± 24 Nmm), also in the range of previous results.

3.2.1. H/D exchange

Fig. 4 shows an example of the behaviour of the O–H stretching profile during deuteration. The intensity of this O–H stretching band decreases in the course of deuteration and it is accompanied by subsequent intensity increasing of the O–D stretching band centred near 2500 cm^{-1}. This spectral behaviour also involves frequency downshifting of the unexchanged O–H stretching band, which occurs

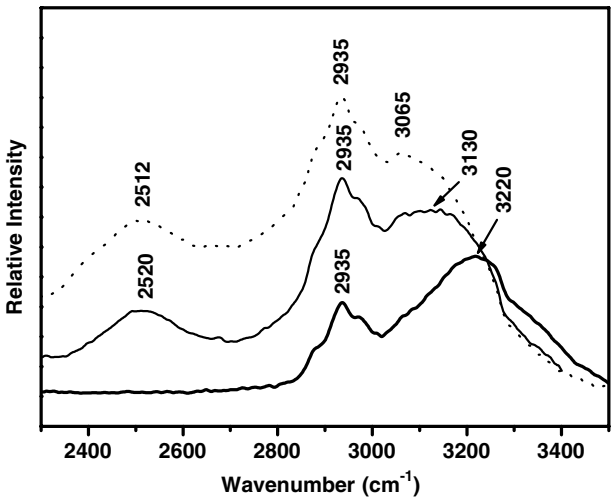

Fig. 4. Raman measurement of H/D exchange for Southern blue whiting (*Micromesistius australis*) gels at 0 (thick line), 3 (thin line), and 7 (dotted line) hours.

Table 3
C–H stretching (expressed as normalized intensity against 1003 cm^{-1} band), relative 3220/3440 cm^{-1} intensity ratio, O–H stretching intensities at 3185, 3160, and 3140 cm^{-1} (expressed as relative intensity to the maximum of the O–H stretching band) and tyrosine doublet ratio I_{850}/I_{830} results (mean ± SEM) in Alaska pollock (*Theragra chalcogramma*) surimi, sol and gel

Samples	C–H stretching	O–H stretching				I_{850}/I_{830}
		I_{3220}/I_{3400}	I_{3185}	I_{3160}	I_{3140}	
Surimi	37.13 ± 2.61^a	4.3 ± 0.2^a	0.77 ± 0.01^a	0.67 ± 0.01^a	0.57 ± 0.04^a	0.66 ± 0.06^a
Sol	34.71 ± 0.80^a	3.90 ± 0.05^a	0.77 ± 0.02^a	0.66 ± 0.01^a	0.55 ± 0.03^a	0.43 ± 0.05^a
Gel	34.6 ± 1.9^a	3.80 ± 0.02^a	0.71 ± 0.02^a	0.55 ± 0.01^a	0.52 ± 0.03^a	0.44 ± 0.05^a

Different letters for the same parameter indicate significant differences ($P < 0.05$).

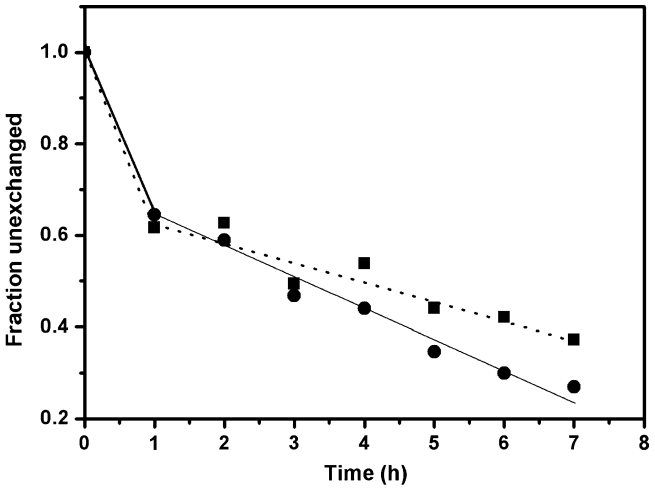

Fig. 5. Fraction of unexchanged O–H groups as a function of H/D exchange time for *Micromesistius australis* surimi (●) and gel (■). Results expressed as relative O–H/C–H stretching area with the area ratio at time zero as absolute value (1.0).

also in surimi samples (results not shown). This frequency shifting is indicative of the presence of water molecular species that are bound with different hydrogen bonding strengths, these being stronger for lower frequencies, and hence the water in the gel generates different H/D exchange kinetics.

The H/D exchange kinetics, expressed as the fraction of unexchanged water O–H bonds versus time, is slightly different for surimi and gel (Fig. 5). Particularly, it should be noticed during the first hour of isotopic exchange, that there are rapid kinetics without significant differences for both types of samples. Thereafter, the deuterations showed exchange rates which are different for surimi and gel and can be fitted to linear equations, as described in the following. The slope of the linear regression equation for gel ($y = 0.67 - 0.043x$; $R^2 = 0.89$, x being the deuteration time) was found to be lower than that of surimi ($y = 0.69 - 0.065x$; $R^2 = 0.97$), and therefore the H/D exchange kinetics in the gel is slower than in surimi.

3.2.2. Microstructure analysis

Raman measurements aimed at determining water domain sizes through the relative intensities at 3200 and 3400 cm^{-1} are valid for domain sizes below 15 nm (Lafleur et al., 1989). Consequently, and in order to explain the H/D kinetics, it is necessary to know the microstructure differences between surimi and gel above the said size. In this connection, we have taken micrographs with various amplifications and seen that the average size of cavities that can enclose water are smaller in gel when compared with surimi. An exemplary image is shown in Fig. 6.

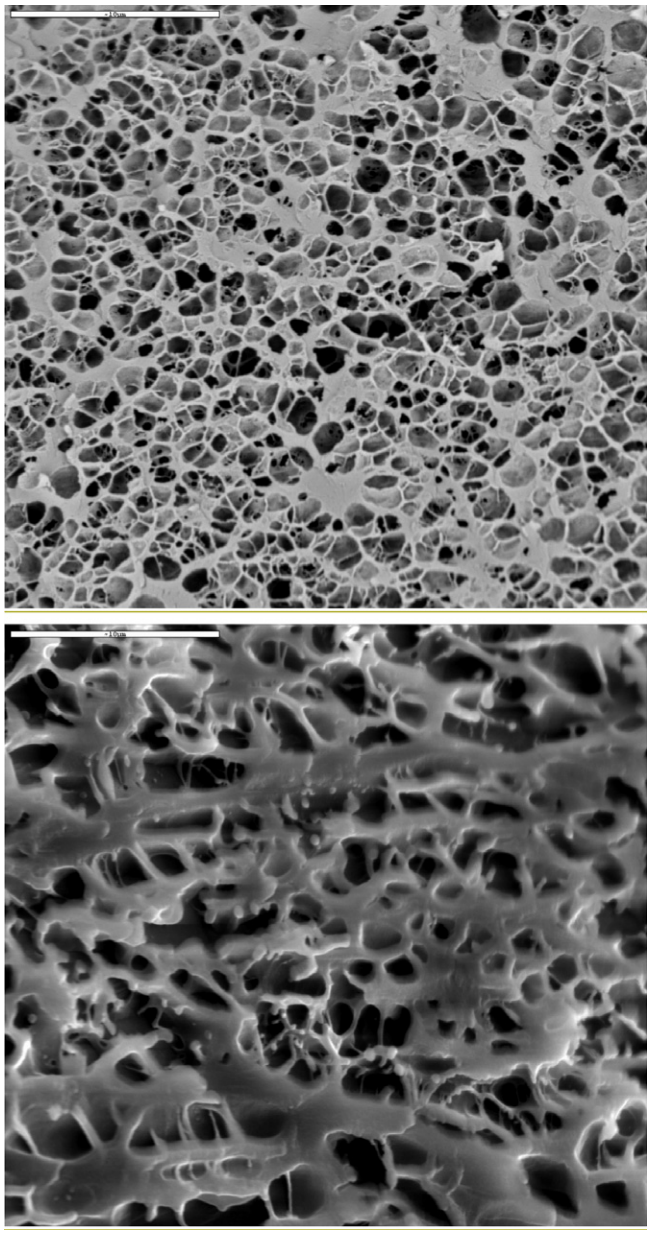

Fig. 6. LT-SEM image of fish surimi (lower) and gel (upper) (5000x).

4. Discussion

We have obtained here, gels having physical-chemical characteristics that are similar to those of gels reported in the literature (Munizaga & Barbosa-Cánovas, 2004; Sánchez-Alonso et al., 2006). The stress relaxation, showed that gels had a higher density of cross-links than the surimi, and also a higher proportion of permanent cross-links, as expected for a gelation process which entails the formation of a three-dimensional protein network structure. The higher viscosity in the two first exponential terms in the gels, can be attributed to entanglement of protein chains and to dissociation and reassociation of non covalent bonds as the proteins slide past each other (Hamann & MacDonald, 1992). Additionally, the time dependent characteristics could also be due to the release of hydraulic pressure induced within the gel specimens during loading (Tang, Tung, & Zeng, 1998).

As to the presence of non covalent cross-links, Raman spectroscopy can provide information in connection with

certain protein conformational transitions occurring during the development and stabilisation of the gel network. We have observed protein structural changes involving hydrophobic interactions in the gelation process (Table 3), but mainly hydrogen bond rearrangements of protein backbone (Fig. 2) in agreement with other works (Bouraoui et al., 1997; Niwa & Hamada, 1981). The FT-Raman spectra of these samples do not allow to confirm the involvement of disulfide S–S bridges and the local changes of the aromatic protein side chains that were observed by other authors (Bouraoui et al., 1997). This may be due either to the raw materials or to different instrument sensitivities, for instance FT instruments as compared with dispersive ones.

The percentage decrease of α-helix structure is an indicator of a partial denaturation of the proteins, rearranged to form a three dimensional structure (Nishinari, Zhang, & Ikeda, 2000). This change can be considered as a net effect of denaturation, because it has been shown that the α-helical structure of gels can be partly recovered upon cooling (Niwa, Nakayama, & Hamada, 1985). According to this interpretation, there is a higher net denaturation of proteins upon the sol-gel transition than through the surimi-sol. The rearrangement of protein secondary structure has been reported to have a role on the stabilization of the gels upon cooling (Lanier et al., 2005; Niwa, 1992). The increase in β-sheet content observed here could, hence, be the result of the changes during the gelling process and the gel stabilization occurring at low temperatures, since these gels were kept chilled for 12 h before analysis. On the other hand, as the temperature is increased upon cooking, coagulation of proteins takes place, resulting in a release of a portion of the water bound by the surimi sol (Niwa, 1992). This author suggested a relationship between the liberation of bound water from the random coil peptide carbonyl group and formation of β-sheet upon heating to high temperature.

Water is necessary to maintain or modify the texture characteristics of gels. Its organization in any polymer solution is variable and dependent on the crosslinking degree, whereby there may be water of protein hydration, interstitial water located in the domains surrounded by protein chains, and free or bulk water (Walrafen & Fisher, 1986). There exists, relatively less studies on water structure in surimi gels as compared with that of proteins, in spite of the important role of intra and intermolecular interactions of water molecules in the formation of these gels (Niwa, 1992; Ahmad, Tashiro, Matsukawa, & Ogawa, 2004; Ahmad, Tashiro, Matsukawa, & Ogawa, 2005). The results included in Table 3 are indicative of changes in the sizes of water domains (3200/3400 cm^{-1} band) below 15 nm, which tend to be smaller in the gel, as well as of weaker strength of water hydrogen bonds in the gels (3185, 3160, 3140 cm^{-1}).

In order to interpret the above results, a second series of experiments was carried out where H/D exchange kinetics has been measured. The WHC (Table 1) changes would be consistent with higher protein-water interaction and/or smaller interstitial water domains. However, it involves water losses due to centrifugation only between 4 and 8%, whereas H/D exchange in these experimental conditions comprises water deuteration fractions reaching 60–70%, and consequently we obtain more complete information on the behaviour of all water types in the course H/D exchange. It is well known that the O–D stretching band appears at lower frequencies (around 2500 cm^{-1}) than those of the O–H stretching band (3200–3500 cm^{-1}). The slowest kinetics of disappearance of the latter in the gels can be explained in terms of stronger water hydrogen bonds, and/or smaller interstitial space domains (Fig. 5). Both WHC and H/D exchange could be interpreted in terms of either of both scenarios: water in these gels being physically trapped and difficult to be extracted by centrifugal forces in the gels, or more tightly bound to proteins. The LT-SEM micrographs show smaller network cavities, which can surround water domains, as compared with those appearing in the surimi image (Fig. 6), which would be consistent with more physically trapped water in the gels having water domains of this magnitude. Moreover, (a) the relative intensities at 3185, 3160 and 3140 cm^{-1} do not seem to indicate that the strength of water hydrogen bonding is higher in these gels, and (b) the increased β-sheet formation could be the result of less protein-water interaction, as described above. Therefore, the results of H/D exchange and WHC should be attributed to a greater inaccessibility of water due to size decreasing of interstitial water domains.

5. Conclusions

The changes found here from surimi to sol and gels in relation to protein structures, refer to decreasing of α-helical structure and concomitant increasing of β-sheets, this transition involving rearrangement of protein hydrogen bonding in agreement with the findings reported by other authors in similar experimental conditions. Part of these changes may contribute to the increase in the viscous and elastic moduli in going from surimi to the gel.

The experiments suggest that the water is more trapped within the gel protein matrix, due to formation of smaller interstitial water domains rather than to stronger water hydrogen bonding to proteins. The method used here for H/D exchange can be applied to study the structural organization of water in surimi products prepared under different conditions or with ingredients that can modify the water-protein interactions and/or the three dimensional structure of the protein networks.

Acknowledgements

This work was performed within the Integrated Project SEAFOODplus, partially granted by the European Union under contract No 506359 and the Spanish Ministerio de Educación y Ciencia under project AGL2002-04104-C04-03. The authors (I.S.-G. and A.R.-C.) thank the CSIC

for financing I3P grants (European Social Foundation). Our thanks are also due to the electron microscopy service of the Instituto de Ciencias Medioambientales (CSIC).

References

Ahmad, M., Tashiro, Y., Matsukawa, S., & Ogawa, H. (2004). Comparison of gelation mechanism of surimi between heat and pressure treatment by using rheological and NMR relaxation measurements. Food Engineering and physical properties. *Journal of Food Science, 69*, E497–E501.

Ahmad, M., Tashiro, Y., Matsukawa, S., & Ogawa, H. (2005). Comparison of horse mackerel and tilapia surimi gel based on rheological and H NMR relaxation properties. *Fisheries Science, 71*, 655–661.

Alix, A. J. P., Pedanou, G., & Berjot, M. (1988). Determination of the quantitative secondary structure of proteins by using some parameters of the Raman amide I band. *Journal of Molecular Structure, 174*, 159–164.

An, H., Peters, M. Y., & Seymour, T. A. (1996). Roles of endogenous enzymes in surimi gelation. *Trends in Food Science & Technology, 7*, 321–326.

AOAC (1995). In P. Cunnif (Ed.), *Official methods of analysis of the association of official agricultural chemists* (16th ed., pp. 7–8). Gaithersburg, Maryland, USA: AOAC International, Ch. 39.

Bouraoui, M., Nakai, S., & Li-Chan, E. (1997). In situ investigation of protein structure in Pacific whiting surimi and gels using Raman spectroscopy. *Food Research International, 30*, 65–72.

Careche, M., Herrero, A., Rodriguez-Casado, A., Del Mazo, M. L., & Carmona, P. (1999). Structural changes of hake fillets: effects of freezing and frozen storage. *Journal of Agricultural and Food Chemistry, 47*, 952–959.

Frushour, B. G., & Koening, J. (1975). Raman spectroscopy of proteins. In R. J. H. Clark & R. E. Hester (Eds.). *Advances in infrared and Raman spectroscopy* (Vol. 2, pp. 35–97). London: Heyden.

Hamann, D. D., & MacDonald, G. A. (1992). Rheology and texture properties of surimi and surimi-based products. In T. C. Lanier & C. Lee (Eds.), *Surimi technology* (pp. 429–500). New York: Marcel Dekker.

Herrero, A., Carmona, P., & Careche, M. (2004). Raman spectroscopic study of structural changes in hake muscle proteins during frozen storage. *Journal of Agricultural and Food Chemistry, 52*, 2147–2153.

Herrero, A., Carmona, P., Garcia, M. L., Solas, M., & Careche, M. (2005). Ultraestructural changes and structure mobility of myowater in frozen-stored hake muscle: relationship with functionality and texture. *Journal of Agricultural and Food Chemistry, 53*, 2558–2566.

Lafleur, M., Pigeon, M., Pézolet, M., & Caillé, J. P. (1989). Raman spectrum of interstitial water in biological systems. *The Journal of Physical Chemistry, 93*, 1522–1526.

Lanier, T. C., Carvajal, P., & Yongsawatdigul, J. (2005). Surimi gelation chemistry. In J. W. Park (Ed.), *Surimi and surimi seafood* (pp. 267–324). New York: Marcel-Dekker.

Lanier, T., Hart., K., & Martin, R. (1991). National Fisheries Institute. A manual of standard methods for measuring and specifying the properties of surimi, Technical subcommittee of the surimi and surimi seafoods, National Fisheries Institute, Washington.

Li-Chan, E., Nakai, S., & Hirotsuka, M. (1994). Raman spectroscopy as a probe of protein structure in food systems. In R. Y. Yada, R. Jackman, & J. L. Smith (Eds.), *Protein structure–function relationships in foods* (pp. 163–197). London U.K: Backie academic & professional, Chapman & Hall.

Lippert, J. L., Tyminski, D., & Desmules, P. (1976). Determination of the secondary structure of proteins by laser Raman Spectroscopy. *The Journal of American Chemistry Society, 98*, 7075–7080.

Maeda, Y., & Kitano, H. (1995). The structure of water in polymer systems revealed by Raman spectroscopy. *Spectrochimica Acta, 51*, 2433–2446.

Mohsenin, N. N. (1970). Some basic concepts of rheology. In *Physical properties of plants and animals materials. Structure, physical characteristics and mechanical properties* (Vol. 1, pp. 832–855). New York: Gordon and Breanch Science Publishers.

Moosavi-Nasab, M., All, I., Ismail, A., & Ngadi, M. (2005). Protein structural changes during preparation and storage of surimi. *Food and Chemical Toxicology, 70*, C448–C453.

Munizaga, G. T., & Barbosa-Cánovas, G. V. (2004). Colour and textural parameters of pressurized and heat-treated surimi gels as affected by potato starch and egg white. *Food Research International, 37*, 767–775.

Nishinari, K., Zhang, H., & Ikeda, S. (2000). Hydrocolloid gels of polysaccharides and proteins. *Current Opinion of Colloids and Interface Science, 5*, 195–201.

Niwa, E. (1992). Chemistry of surimi gelation. In T. C. Lanier & C. Lee (Eds.), *Surimi technology* (pp. 389–427). New York: Marcel Dekker.

Niwa, E., & Hamada, I. (1981). Supplementary Studies on the presence of β structure in fish flesh gel. *Bulletin of the Japanese Society of Scientific Fisheries, 47*, 1091.

Niwa, E., Nakayama, T., & Hamada, I. (1985). Secondary structural change in protein during processing fish flesh gel. *Nippon Suisan Gakkaishi, 51*, 855.

Ogawa, M., Nakamura, S., Horimoto, Y., An, H., Tsuchiya, T., & Nakai, S. (1999). Raman spectroscopy study of changes in fish actomyosin during setting. *Journal of Agricultural and Food Chemistry, 47*, 3309–3318.

Roussel, H., & Cheftel, J. (1990). Mechanisms of gelation of sardine proteins: influence of thermal processing and of various additives on the texture and protein solubility of kamaboko gels. *International Journal of Food Science & Technology, 25*, 260–280.

Sammon, C., Bajwa, G., Timmins, P., & Melia, C. (2006). The application of attenuated total reflectance Fourier transform infrared spectroscopy to monitor the concentration and state of water in solutions of a thermally responsive cellulose ether during gelation. *Polymer, 47*, 577–584.

Sánchez-Alonso, I., Haji-Maleki, R., & Borderías, J. (2006). Effect of wheat fibre in frozen stored fish muscular gels. *European Journal of Food Research and Technology, 223*, 571–576.

Scherer, J. R. (1980). The vibrational spectroscopy of water. In R. J. H. Clark & R. E. Hester (Eds.). *Advances in infrared and Raman spectroscopy* (Vol. 5). London: Heyden.

Siamwiza, M. N., Lord, R. C., Chen, M. C., Takamatsu, T., Harada, I., Matsuura, et al. (1975). Interpretation of the doublet at 850 and 830 cm^{-1} in the Raman spectra of tyrosyl residues in proteins and certain model compounds. *Biochemistry, 14*, 4870–4876.

Stone, A., & Stanley, D. (1992). Mechanisms of fish muscle gelation. *Food Research International, 25*, 381–388.

Tang, J., Tung, M. A., & Zeng, Y. (1998). Characterization of gellan gels using stress relaxation. *Journal of Food Engineering, 38*, 279–295.

Thawornchinsombut, S., Park, J. W., Meng, G. T., & Li-Chan, E. C. Y. (2006). Raman spectroscopy determines structural changes associated with gelation properties of fish proteins recovered at alkaline pH. *Journal of Agricultural and Food Chemistry, 54*, 2178–2187.

Tu, A. T. (1982). Proteins. In A. T. Tu (Ed.), *Raman spectroscopy in biology*. New York: Wiley.

Uresti, R. M., López-Arias, N., González-Cabriales, J., Ramirez, J., & Vázquez, M. (2003). Use of amidated low methoxyl pectin to produce fish restructured products. *Food Hydrocolloids, 17*, 171–176.

Walrafen, G. E., & Fisher, M. (1986). Low-frequency Raman scattering from water and aqueous solutions: A direct measure of hydrogen Bonding. *Methods in Enzymology, 127*, 91–105.

Yu, T. S., Lippert, J. L., & Peticolas, W. (1973). Laser Raman studies of conformational variations of poly-L-lysine. *Biopolymers, 12*, 2161–2176.